NANO LETTERS

Letter

pubs.acs.org/NanoLett

Vertical Heterostructure of Two-Dimensional MoS_2 and WSe_2 with Vertically Aligned Layers

Jung Ho Yu,[†] Hye Ryoung Lee,[‡] Seung Sae Hong,[§] Desheng Kong,[†] Hyun-Wook Lee,[†] Haotian Wang,[§] Feng Xiong,[‡] Shuang Wang,[‡] and Yi Cui*[,∥,†]

[†]Department of Materials Science and Engineering, [‡]Department of Electrical Engineering, and [§]Department of Applied Physics, Stanford University, Stanford, California 94305, United States

[∥]Stanford Institute for Materials and Energy Sciences, SLAC National Accelerator Laboratory, 2575 Sand Hill Road, Menlo Park, California 94025, United States

Supporting Information

ABSTRACT: Two-dimensional (2D) layered materials consist of covalently bonded 2D atomic layers stacked by van der Waals interactions. Such anisotropic bonding nature gives rise to the orientation-dependent functionalities of the 2D layered materials. Different from most studies of 2D materials with their atomic layers parallel to substrate, we have recently developed layer vertically aligned 2D material nanofilms. Built on these developments, here, we demonstrate the synthesis of vertical heterostructure of n-type MoS_2 and p-type WSe_2 with vertically aligned atomic layers. Thin film of MoS_2/WSe_2 vertical structure was successfully synthesized without significant alloy formation. The heterostructure synthesis is scalable to a large area over 1 cm^2. We demonstrated the pn junction diode behavior of the heterostructure device. This novel device geometry opens up exciting opportunities for a variety of electronic and optoelectronic devices, complementary to the recent interesting vertical heterostructures with horizontal atomic layers.

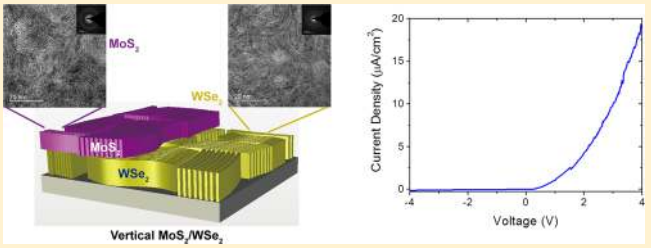

KEYWORDS: *Two-dimensional layered material, transition metal dichalcogenide, heterostructure, molybdenum disulfide, tungsten diselenide, vertically aligned layer*

Two-dimensional (2D) layered materials are a unique class of materials in which two-dimensional covalently bonded atomic layers are stacked by van der Waals interactions.[1] Such anisotropic bonding nature enabled to manipulate materials properties in unique ways. For example, intercalation of ions,[2] atoms,[3,4] and molecules between atomic layers induces electrical, optical, and structural changes in the host layered materials,[5,6] while exfoliation provides a facile method to yield 2D materials with one or a few atomic layers.[7,8] Two-dimensional transition metal dichalcogenides such as molybdenum disulfide (MoS_2) and tungsten diselenide (WSe_2) are intriguing because their semiconducting properties can be tailored in the engineering methods of 2D layered materials.[9−11] For example, the exfoliation method allows observation of indirect to direct band gap transition, when the exfoliated atomic layer approaches to monolayer.[12,13] Furthermore, the 2D layered materials can build-up heterostructure by stacking the van der Waals layers in direction perpendicular to the atomic layer.[14] The exploration of the 2D layered material heterostructure is currently on the way,[15−22] and the atomic layer pn junction between n-type MoS_2 and p-type WSe_2 was reported very recently.[16]

Different from those layer horizontally lying 2D materials, we have recently developed layer vertically aligned 2D material nanofilms, exposing their edge sites in a maximized manner. These nanofilms were synthesized via kinetically controlled growth through rapid sulfurization and selenization of the corresponding metal films.[23−26] We have demonstrated the edge-exposed structure of MoS_2 with vertically aligned 2D atomic layers is an excellent platform for hydrogen evolution reaction (HER) catalyst.[23] The edge-exposed 2D layered materials can be synthesized on various substrates including silicon nanowire and carbon fiber paper.[24] Their properties can be further engineered via Li intercalation electrochemical tuning, which controls oxidation state, doping, and phase of the materials.[25]

To expand such an orientation control in functionalities of the edge-exposed 2D materials with vertically aligned layers, it is essential to combine the different materials into one heterostructure in vertical direction. Especially, WSe_2 and MoS_2 are semiconductors with p-type and n-type, respectively.[27−29] The combination of the materials is of particular importance owing to their high band offsets among transition metal dichalcogenide semiconductors[29] and will create pn junction diode, which is a basic component for semiconductor electronic circuits. Here we report scalable synthesis of vertical heterostructure of MoS_2/WSe_2 with vertically aligned 2D layers

Received: October 10, 2014
Revised: December 26, 2014

DOI: 10.1021/nl503897h
Nano Lett. XXXX, XXX, XXX−XXX

and large area pn junction diode based on the heterostructure. Our heterostructures with vertically aligned 2D layers are different from those recently reported heterostructures with horizontally lying layers.

Vertical heterostructure of WSe_2 and MoS_2 with vertically aligned layers was synthesized from sequential growth of WSe_2 and MoS_2 via kinetically controlled rapid selenization and sulfurization, respectively (Figure 1). The synthesis begins with

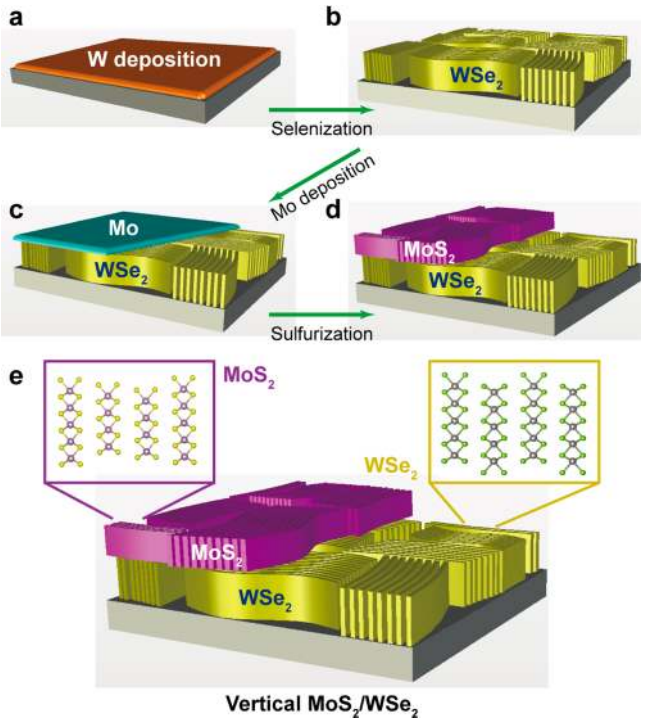

Figure 1. Schematics of MoS_2/WSe_2 vertical heterostructure synthesis. (a) Tungsten (W) is coated onto the substrate. (b) WSe_2 film with vertically aligned layer is formed via rapid selenization. (c) Molybdenum (Mo) is coated on top of the synthesized WSe_2 film. (d) MoS_2/WSe_2 vertical heterostructure is formed via rapid sulfurization. (e) The heterostructure consists of the MoS_2 and WSe_2, in which their van der Waals layers are aligned perpendicular to the substrate.

rapid selenization of 30 nm thick tungsten film at 600 °C to produce 100 nm thick edge-exposed WSe_2 film (Figures 1a,b and 2). Dark-field scanning transmission electron microscope image (STEM, Figure 2a) and the corresponding elemental maps of the film (Figure 2b) shows that WSe_2 was successfully synthesized from the selenization of the tungsten thin-film. It should be noted that while the yield of MoS_2 with vertically aligned layers approaches 100% over wide range of temperature and pressure,[23] the yield of WSe_2 with vertically aligned layers is dependent on the carrier gas pressure (Supporting Information Figure S1). At argon carrier gas pressure of 10 Torr, we obtained WSe_2 with vertically aligned layers with over 85% yield, which was calculated from the edge-exposed area observed from a transmission electron microscope (TEM) (Figure 2c). The synthesized WSe_2 is polycrystalline with their average domain size of ~20 nm. The polycrystalline nature of WSe_2 with vertically aligned layers is further supported by the corresponding selected-area electron diffraction pattern (inset of Figure 2c). After the successful synthesis of WSe_2 with vertically aligned layers, 15 nm thick molybdenum thin film was coated on top of the edge-exposed WSe_2 film by sputtering (Figure 1c). Subsequently, Mo/WSe_2 thin film was rapidly sulfurized at 600 °C to produce MoS_2/WSe_2 140 nm thick heterostructure (Figure 1d). TEM image shows a homogeneous thin film was created after the sulfurization (Figure 3a). The elemental maps of the film show the homogeneous thin film is composed of W, Se, Mo, and S (Figure 3b), while the previously formed WSe_2 film is composed of only W and Se (Figure 2b and Supporting Information Figure S2). As the TEM characterization is conducted from the top-view of the film, the sulfurization product of Mo/WSe_2 is visualized rather than WSe_2, which is now placed on the bottom side of the film. The higher magnification TEM image shows the polycrystalline edge-exposed structure is retained after sulfurization of Mo/WSe_2 (Figure 3c), implying the production of MoS_2 with vertically aligned 2D layers on top of the edge-terminated WSe_2 (Figure 1e).

The MoS_2/WSe_2 heterostructure formation is further confirmed by Raman spectroscopy (Figure 4a). The synthesized heterostructure film clearly shows spectral features of both edge-terminated MoS_2 and WSe_2. When edge-terminated two-dimensional dichalcogenides (MX_2) were grown in a way that the van der Waals layers are aligned vertically to substrates, the out-of-plane M−X vibration mode (A_{1g}) is expected to dominate over in-plane M−X vibration mode (E^1_{2g}). This spectral signature is hard to be resolved in the Raman spectrum of WSe_2 (Figure 4a, red) because of the small energy difference between A_{1g} mode (253 cm^{-1}) and E^1_{2g} (250 cm^{-1}).[30]

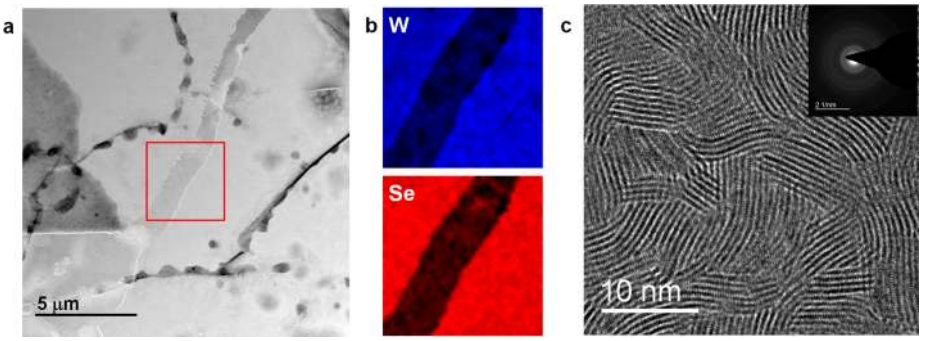

Figure 2. TEM characterization of WSe_2 with vertically aligned 2D layers. (a) Low-magnification dark-field scanning transmission electron microscope (STEM) image of WSe_2 film on carbon grid. (b) Elemental maps of the WSe_2 film, obtained from an EDX scan of the red rectangular area in panel a. (c) High-magnification TEM image of the WSe_2 film with vertically aligned layers. The inset shows the corresponding electron diffraction (ED) pattern of the WSe_2 film.

DOI: 10.1021/nl503897h
Nano Lett. XXXX, XXX, XXX−XXX

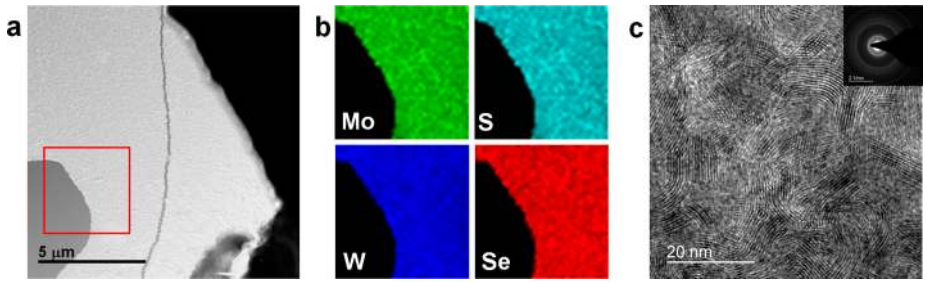

Figure 3. TEM characterizations of MoS_2/WSe_2 vertical heterostructure. (a) Low-magnification dark-field scanning transmission electron microscope (STEM) image of the MoS_2/WSe_2 thin-film. (b) Elemental maps of the MoS_2/WSe_2 thin film. The images were obtained from an EDX scan of the red rectangular region in panel a. (c) High-magnification TEM image of MoS_2/WSe_2 thin-film, which clearly shows vertically aligned van der Waals layers of the MoS_2/WSe_2 heterostructure. The inset shows the corresponding electron diffraction (ED) pattern of the MoS_2/WSe_2 heterostructure.

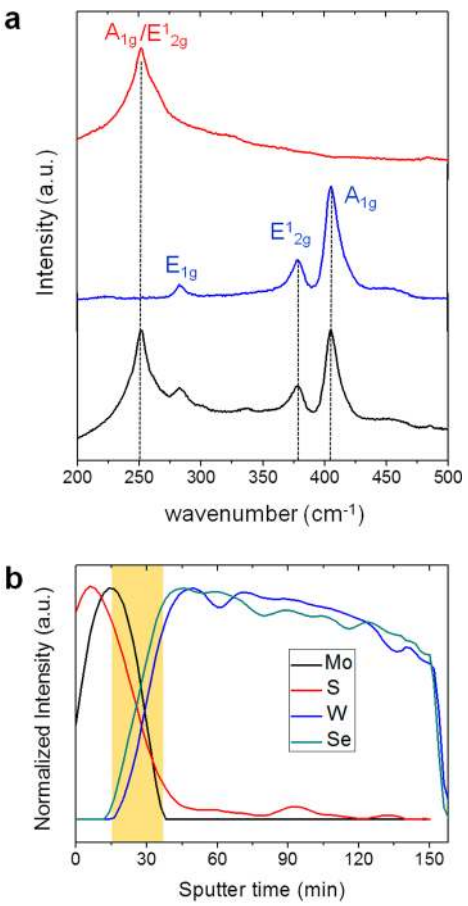

Figure 4. Characterization of MoS_2/WSe_2 heterostructure. (a) Raman spectra of WSe_2 (red), MoS_2 (blue), and MoS_2/WSe_2 heterostructure (black). (b) Depth-resolved elemental profile of molybdenum (black), sulfur (red), tungsten (blue), and selenium (green), obtained from scanning Auger electron spectroscopy. The profile was obtained in every 2 min interval, with continuous etching of the MoS_2/WSe_2 film by 1 kV Ar plasma. The yellow mark indicates the intermixing region in which Mo, S, W, and Se are simultaneously detected from the spectra.

Meanwhile, it is clearly indicated from the Raman spectrum of MoS_2 (Figure 4a, blue) in which Raman peak intensity of A_{1g} mode (408 cm^{-1}) is stronger than that of E^1_{2g} mode (383 cm^{-1}).[23,31] In the Raman spectrum of the synthesized heterostructure of MoS_2/WSe_2 (Figure 4a, black), it is clarified not only the existence of both MoS_2 and WSe_2 in a film but also the spectral feature of the edge-terminated MoS_2. If MoS_2 and WSe_2 undergo alloying, the in-plane M−X vibration mode (E_{1g} and E^1_{2g}) of MoS_2 shifts to lower frequency, while that of WSe_2 shifts to higher frequency. The frequency shift is originated from the atomic weight difference of both constituent cations (Mo and S) and anions (S and Se).[32] However, the A_{1g} vibration mode of MoS_2, in which only anion atoms vibrate in out-of-plane direction, is pure indicator of anion alloying and therefore should move to lower frequency when alloying between sulfur and selenium atoms occurs. In our Raman spectra, there is no difference between E_{1g} and A_{1g} mode of the separately synthesized MoS_2 and WSe_2 and that of the MoS_2/WSe_2. There is only 6 cm^{-1} difference in E^1_{2g} mode of the MoS_2 and that of the MoS_2/WSe_2, which corresponds to 0.7 meV and is negligible. This implies that there is no significant alloying of MoS_2 and WSe_2 undergone in the synthetic condition.

We also conducted scanning Auger electron spectroscopy, which provides the depth-resolved elemental profile of the MoS_2/WSe_2 heterostructure film (Figure 4b and Supporting Information Figure S3). The existence of four component elements of molybdenum, sulfur, tungsten, and selenium were quantified with continuous etching of the heterostructure by Ar ion from top to bottom direction. In this way, the top-layer of MoS_2 was analyzed first, and then the bottom-layer of WSe_2 was analyzed after complete etching of the MoS_2 layer. From the depth-resolved elemental profile, it was only 13% of the film, in which all four component elements were detected in the spectra (yellow zone in Figure 4b). This overlap zone is estimated as 18 nm in thickness, where the surface roughness (9 nm) of the bottom WSe_2 layer and the depth resolution (∼15 nm) of Auger spectroscopy profiling can contribute to this variation. This implies that the degree of interdiffusion of the component elements is only limited to the boundary between MoS_2 and WSe_2. Both the Raman spectra and the Auger electron spectroscopy depth-profile clearly indicate that no significant alloying occurs in the MoS_2/WSe_2 heterostructure synthesis condition.

In the heterostructure synthesis, the scalability of the synthesis is only limited to the area of the selenizing or sulfurizing metal film. Therefore, the synthesis is scalable to a large area, when large area thin-film of W and Mo are employed in the synthesis (Figure 5a). Furthermore, the large area heterostructure film can be transferred to various substrates by simple polymer-based transfer method (Figure 5a and Supporting Information). On the basis of the MoS_2/WSe_2 vertical heterostructure, we fabricated the sandwich structure device in which Pd was contacted with WSe_2 as a positive

DOI: 10.1021/nl503897h
Nano Lett. XXXX, XXX, XXX−XXX

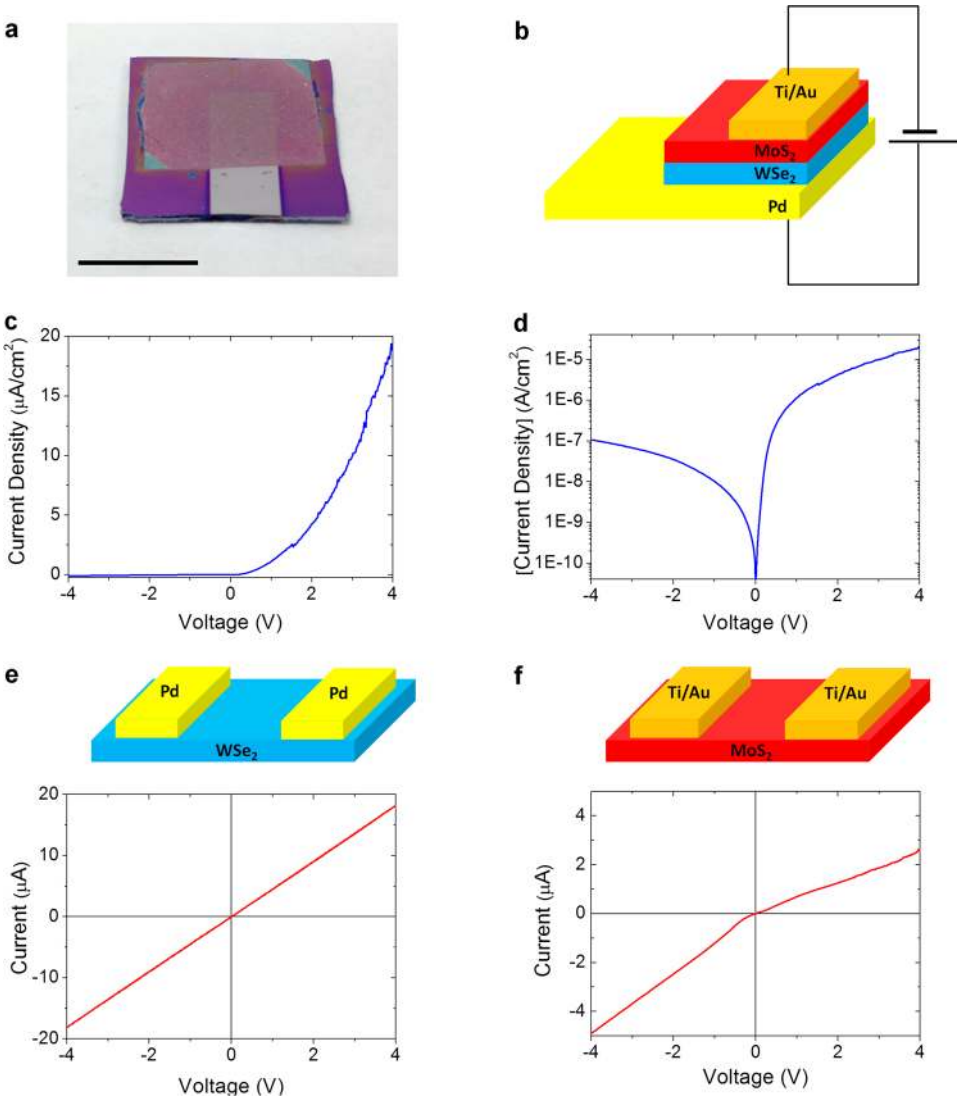

Figure 5. Heterostructure film transfer and transport measurement of the MoS_2/WSe_2 heterostructure. (a) Transferred MoS_2/WSe_2 heterostructure film on a Pd electrode pad. The dimension of the pad is 2 cm × 2 cm. Scale bar, 1 cm. (b) Schematic of the MoS_2/WSe_2 heterostructure diode. The heterostructure was sandwiched between Pd and Ti/Au, which were defined as positive and negative electrodes, respectively. (c) Current−voltage characteristic of the MoS_2/WSe_2 heterostructure diode. (d) Logarithmic plot of the current−voltage curve in panel c. (e) Schematic and current−voltage characteristic of WSe_2 thin film two-terminal device on which Pd electrodes were placed. (f) Schematic and current−voltage characteristics of MoS_2 thin film two-terminal device on which Ti/Au electrodes were placed.

electrode and Ti/Au was contacted with MoS_2 as a negative electrode (Figure 5b). Current−voltage characteristic curve of the device shows typical diode characteristic with ON/OFF current ratio of ∼150 and ideality factor of 1.5 at lower voltage range below 1 V (Figure 5c,d). To elucidate the origin of the diode characteristic, we separately made the two-terminal devices of Pd−WSe_2−Pd and Ti/Au−MoS_2−Ti/Au (Figure 5e,f). The current−voltage characteristic curves of both two-terminal devices show nearly an ohmic characteristic. It has been known that MoS_2 is an intrinsic n-type semiconductor,[27] while WSe_2 is an intrinsic p-type semiconductor.[28] Therefore, it is concluded that the rectification behavior of the device is originated from the pn junction between n-type MoS_2 and p-type WSe_2. In the vertical pn junction diode of MoS_2/WSe_2 with vertically aligned van der Waals layers, the ON/OFF current ratio is high enough. However, the absolute value of the ON current density is small, compared to previously reported high-purity polycrystalline heterostructure synthesized over 1000 °C.[33] It is speculated that charge carrier hopping across polycrystalline domain within edge-terminated MoS_2 and WSe_2 layers is still a dominant carrier transport mechanism, although the average current flow of the heterostructure diode is toward the in-plane direction of the 2D atomic layer.

In conclusion, we have demonstrated scalable synthesis of vertical heterostructure of MoS_2/WSe_2 with vertically aligned 2D layers. Homogeneous thin film of MoS_2/WSe_2 vertical structure was successfully synthesized without significant alloy formation. Furthermore, the heterostructure synthesis is scalable to a large area over 1 cm^2. We also demonstrated a pn junction diode based on the heterostructure. The heterostructure described here is an excellent platform to exploit both science and engineering aspects of the two-dimensional dichalcogenide materials. For example, it is known that WSe_2 is a decent light-absorber,[34] while the edge-site of MoS_2 can be used for catalysts for various chemical reactions including hydrogen-evolution reaction (HER). We expect that

DOI: 10.1021/nl503897h
Nano Lett. XXXX, XXX, XXX−XXX

adopting those functionalities to the MoS_2/WSe_2 vertical heterostructure will provide an excellent model of novel photocathode for water splitting.

■ ASSOCIATED CONTENT

Supporting Information

Additional details on materials synthesis and characterizations, TEM images, EDS spectra, and AES spectra. This material is available free of charge via the Internet at http://pubs.acs.org.

■ AUTHOR INFORMATION

Corresponding Author

*E-mail: yicui@stanford.edu.

Author Contributions

J.H.Y. and Y.C. conceived the idea. J.H.Y. carried out materials synthesis and fabrication of the pn junction diode. J.H.Y., H.R.L., S.S.H., D.K., H.-W.L., H.W., F.X., and S.W. performed materials characterizations. J.H.Y. and Y.C. cowrote the paper. All the authors discussed the results and commented on the manuscript.

Notes

The authors declare no competing financial interest.

■ ACKNOWLEDGMENTS

This work was supported by the Department of Energy, Office of Basic Energy Sciences, Division of Materials Sciences and Engineering, under contract DE-AC02-76SF00515. H.-W.L. was supported by Basic Science Research Program through the National Research Program through the National Research Foundation of Korea (NRF) funded by the Ministry of Education, Science and Technology (no. NRF-2012R1A6A3A03038593).

■ REFERENCES

(1) Butler, S. Z.; Hollen, S. M.; Cao, L.; Cui, Y.; Gupta, J. A.; Gutierrez, H. R.; Heinz, T. F.; Hong, S. S.; Huang, J.; Ismach, A. F.; Johnston-Halperin, E.; Kuno, M.; Plashnitsa, V. V.; Robinson, R. D.; Ruoff, R. S.; Salahuddin, S.; Shan, J.; Shi, L.; Spencer, M. G.; Terrones, M.; Windl, W.; Goldberger, J. E. *ACS Nano* **2013**, *7* (4), 2898−2926.

(2) Whittingham, M. S. *Prog. Solid State Chem.* **1978**, *12* (1), 41−99.

(3) Koski, K. J.; Wessells, C. D.; Reed, B. W.; Cha, J. J.; Kong, D.; Cui, Y. *J. Am. Chem. Soc.* **2012**, *134* (33), 13773−13779.

(4) Koski, K. J.; Cha, J. J.; Reed, B. W.; Wessells, C. D.; Kong, D.; Cui, Y. *J. Am. Chem. Soc.* **2012**, *134* (18), 7584−7587.

(5) Divigalpitiya, W. M.; Frindt, R. F.; Morrison, S. R. *Science* **1989**, *246* (4928), 369−371.

(6) Cha, J. J.; Koski, K. J.; Huang, K. C. Y.; Wang, K. X.; Luo, W.; Kong, D.; Yu, Z.; Fan, S.; Brongersma, M. L.; Cui, Y. *Nano Lett.* **2013**, *13* (12), 5913−5918.

(7) Novoselov, K. S.; Jiang, D.; Schedin, F.; Booth, T. J.; Khotkevich, V. V.; Morozov, S. V.; Geim, A. K. *Proc. Natl. Acad. Sci.* **2005**, *102* (30), 10451−10453.

(8) Coleman, J. N.; Lotya, M.; O'Neill, A.; Bergin, S. D.; King, P. J.; Khan, U.; Young, K.; Gaucher, A.; De, S.; Smith, R. J. *Science* **2011**, *331* (6017), 568−571.

(9) Xu, M.; Liang, T.; Shi, M.; Chen, H. *Chem. Rev.* **2013**, *113* (5), 3766−3798.

(10) Jariwala, D.; Sangwan, V. K.; Lauhon, L. J.; Marks, T. J.; Hersam, M. C. *ACS Nano* **2014**, *8* (2), 1102−1120.

(11) Chhowalla, M.; Shin, H. S.; Eda, G.; Li, L.-J.; Loh, K. P.; Zhang, H. *Nat. Chem.* **2013**, *5* (4), 263−275.

(12) Splendiani, A.; Sun, L.; Zhang, Y.; Li, T.; Kim, J.; Chim, C.-Y.; Galli, G.; Wang, F. *Nano Lett.* **2010**, *10* (4), 1271−1275.

(13) Mak, K. F.; Lee, C.; Hone, J.; Shan, J.; Heinz, T. F. *Phys. Rev. Lett.* **2010**, *105* (13), 136805.

(14) Geim, A. K.; Grigorieva, I. V. *Nature* **2013**, *499*, 419−425.

(15) Fang, H.; Battaglia, C.; Carraro, C.; Nemsak, S.; Ozdol, B.; Kang, J. S.; Bechtel, H. A.; Desai, S. B.; Kronast, F.; Unal, A. A.; Conti, G.; Conlon, C.; Palsson, G. K.; Martin, M. C.; Minor, A. M.; Fadley, C. S.; Yablonovitch, E.; Maboudian, R.; Javey, A. *Proc. Natl. Acad. Sci.* **2014**, *111* (17), 6198−6202.

(16) Lee, C.-H.; Lee, G.-H.; van der Zander, A. M.; Chen, W.; Li, Y.; Han, M.; Cui, X.; Arefe, G.; Nuckolls, C.; Heinz, T. F.; Guo, J.; Hone, J.; Kim, P. *Nat. Nanotechnol.* **2014**, *9* (9), 676−681.

(17) Furchi, M. M.; Pospischil, A.; Libsch, F.; Burgdörfer, J.; Mueller, T. *Nano Lett.* **2014**, *14* (8), 4785−4791.

(18) Hong, X.; Kim, J.; Shi, S.-F.; Zhang, Y.; Jin, C.; Sun, Y.; Tongay, S.; Wu, J.; Zhang, Y.; Wang, F. *Nat. Nanotechnol.* **2014**, *9* (9), 682−686.

(19) Cheng, R.; Li, D.; Zhou, H.; Wang, C.; Yin, A.; Jiang, S.; Liu, Y.; Chen, Y.; Huang, Y.; Duan, X. *Nano Lett.* **2014**, *14*, 5590−5597.

(20) Huang, C.; Wu, S.; Sanchez, A. M.; Peters, J. J. P.; Beanland, R.; Ross, J. S.; Rivera, P.; Yao, W.; Cobden, D. H.; Xu, X. *Nat. Mater.* **2014**, *13*, 1096−1101.

(21) Chiu, M.-H.; Li, M.-Y.; Zhang, W.; Hsu, W.-T.; Chang, W.-H.; Terrones, M.; Terrones, H.; Li, L.-J. *ACS Nano* **2014**, *8* (9), 9646−9656.

(22) Jung, Y.; Shen, J.; Sun, Y.; Cha, J. J. *ACS Nano* **2014**, *8* (9), 9550−9557.

(23) Kong, D.; Wang, H.; Cha, J. J.; Pasta, M.; Koski, K. J.; Yao, J.; Cui, Y. *Nano Lett.* **2013**, *13* (3), 1341−1347.

(24) Wang, H.; Kong, D.; Johanes, P.; Cha, J. J.; Zheng, G.; Yan, K.; Liu, N.; Cui, Y. *Nano Lett.* **2013**, *13* (7), 3426−3433.

(25) Wang, H.; Lu, Z.; Xu, S.; Kong, D.; Cha, J. J.; Zheng, G.; Hsu, P.-C.; Yan, K.; Bradshaw, D.; Prinz, F. B.; Cui, Y. *Proc. Natl. Acad. Sci.* **2013**, *110* (49), 19701−19706.

(26) Wang, H.; Lu, Z.; Kong, D.; Sun, J.; Hymel, T. M.; Cui, Y. *ACS Nano* **2014**, *8* (5), 4940−4947.

(27) Radisavljevic, B.; Radenovic, A.; Brivio, J.; Giacometti, V.; Kis, A. *Nat. Nanotechnol.* **2011**, *6* (3), 147−150.

(28) Fang, H.; Chuang, S.; Chang, T. C.; Takei, K.; Takahashi, T.; Javey, A. *Nano Lett.* **2012**, *12* (7), 3788−3792.

(29) Kang, J.; Tongay, S.; Zhou, J.; Li, J. B.; Wu, J. Q. *Appl. Phys. Lett.* **2013**, *102* (1), 012111.

(30) Mead, D. G.; Irwin, J. C. *Can. J. Phys.* **1977**, *55* (5), 379−382.

(31) Verble, J. L.; Wieting, T. J. *Phys. Rev. Lett.* **1970**, *25* (6), 362−365.

(32) Dumenco, D. O.; Chen, K. Y.; Wang, Y. P.; Huang, Y. S.; Tiong, K. K. *J. Alloys Compd.* **2010**, *506*, 940−943.

(33) Späh, R.; Lux-Stenier, M.; Obergfell, M.; Bucher, E.; Wagner, S. *Appl. Phys. Lett.* **1985**, *47* (8), 871−873.

(34) McKone, J. R.; Pieterick, A. P.; Gray, H. B.; Lewis, N. S. *J. Am. Chem. Soc.* **2013**, *135* (1), 223−231.

DOI: 10.1021/nl503897h
Nano Lett. XXXX, XXX, XXX−XXX